HHS Public Access

Author manuscript

Mol Pharm. Author manuscript; available in PMC 2017 August 04.

Published in final edited form as:

Mol Pharm. 2016 January 04; 13(1): 262–271. doi:10.1021/acs.molpharmaceut.5b00706.

Selective intracellular delivery of recombinant arginine deiminase (ADI) using pH-sensitive cell penetrating peptides to overcome ADI resistance in hypoxic breast cancer cells

Tzyy-Harn Yeh[a,b,‡], **Yun-Ru Chen**[c,‡], **Szu-Ying Chen**[c,d], **Wei-Chiang Shen**[b], **David K. Ann**[c,*], **Jennica L. Zaro**[b,*], and **Li-Jiuan Shen**[a,e,f,*]

[a]School of Pharmacy, College of Medicine, National Taiwan University, Taipei, Taiwan

[b]Department of Pharmacology and Pharmaceutical Sciences, School of Pharmacy, University of Southern California, Los Angeles, CA 90033, USA

[c]Department of Metabolic Research, Beckman Research Institute, City of Hope, Duarte, CA 91010, USA

[d]Department of Medical Laboratory Science and Biotechnology, National Cheng Kung University, Tainan, Taiwan

[e]Graduate Institute of Clinical Pharmacy, College of Medicine, National Taiwan University, Taipei, Taiwan

[f]Department of Pharmacy, National Taiwan University Hospital, Taipei, Taiwan

Abstract

Arginine depletion strategies, such as pegylated recombinant arginine deiminase (ADI-PEG20), offer a promising anticancer treatment. Many tumor cells have suppressed expression of a key enzyme, argininosuccinate synthetase 1 (ASS1), which converts citrulline to arginine. These tumor cells become arginine auxotrophic, as they can no longer synthesize endogenous arginine intracellularly from citrulline, and are therefore sensitive to arginine depletion therapy. However, since ADI-PEG20 only depletes extracellular arginine due to low internalization, ASS1-expressing cells are not susceptible to treatment since they can synthesize arginine intracellularly. Recent studies have found that several factors influence ASS1 expression. In this study, we evaluated the effect of hypoxia, frequently encountered in many solid tumors, on ASS1 expression and its relationship to ADI-resistance in human MDA-MB-231 breast cancer cells. It was found that MDA-MB-231 cells developed ADI resistance in hypoxic conditions with increased ASS1 expression. To restore ADI sensitivity as well as achieve tumor-selective delivery under hypoxia,

*Corresponding authors: Li-Jiuan Shen, Ph.D., Associate Professor, Graduate Institute of Clinical Pharmacy, College of Medicine, National Taiwan University, Taipei, Taiwan, ljshen@ntu.edu.tw, Phone: +886-2-33668792. Jennica L. Zaro, Ph.D., Assistant Professor, University of Southern California, CA, USA, zaro@usc.edu, Phone: 1-323-442-1933. David K. Ann, Ph.D., Professor, Beckman Research Institute, City of Hope, CA, USA, dann@coh.org, Phone: 626-218-4967.

‡THY and YRC contributed equally.

Author Contributions

The manuscript was written through contributions of all authors. All authors have given approval to the final version of the manuscript. THY aided in experimental design, performed experiments and wrote the manuscript. YRC aided in experimental design and performed experiments. SYC aided in performing the PC3 and PBMC experiments. WCS, DKA, JLZ and LJS aided in experimental design, analyzed the data and edited the manuscript.

we constructed a pH-sensitive cell penetrating peptide (CPP)-based delivery system to carry ADI inside cells to deplete both intra- and extracellular arginine. The delivery system was designed to activate the CPP-mediated internalization only at the mildly acidic pH (6.5–7) associated with the microenvironment of hypoxic tumors, thus achieving better selectivity toward tumor cells. The pH sensitivity of the CPP, HBHAc, was controlled by recombinant fusion to a histidine-glutamine (HE) oligopeptide, generating HBHAc-HE-ADI. The tumor distribution of HBHAc-HE-ADI was comparable to ADI-PEG20 in a mouse xenograft model of human breast cancer cells *in vivo*. In addition, HBHAc-HE-ADI showed increased *in vitro* cellular uptake in cells incubated in a mildly acidic pH (hypoxic conditions) compared to normal pH (normoxic conditions), which correlated with pH-sensitive *in vitro* cytotoxicity in hypoxic MDA-MB-231 and human prostate cancer PC3 cells. Together, we conclude that the HBHAc-HE-based peptide delivery offers a useful means to overcome hypoxia-induced resistance to ADI in breast cancer cells, and to target the mildly acidic tumor microenvironment.

Graphical Abstract

Schematic presentation of the selective intracellular delivery of recombinant arginine deiminase (ADI) using pH-sensitive cell penetrating peptides to overcome ADI resistance in hypoxic breast cancer cells MDA-MB-231.

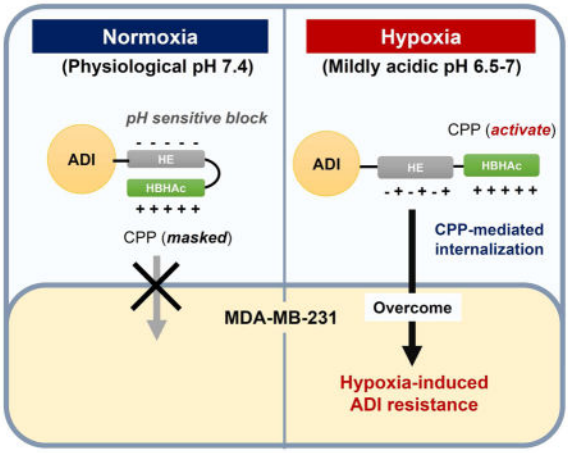

Keywords

hypoxia; pH-sensitive peptide; tumor targeting; argininosuccinate synthetase; arginine deiminase resistance

Introduction

Arginine deiminase (ADI), a *Mycoplasma* enzyme which catalyzes the conversion of arginine into citrulline, is a promising anticancer therapeutic which shows cytotoxicity in arginine-auxotrophic tumors by depleting extracellular arginine and causing cell starvation. The pegylated form, ADI-PEG20, is currently in clinical trials for treating different cancers [1–4]. Due to their low internalization, arginine depletion therapies including ADI and ADI-PEG20 work outside the cell in depleting extracellular arginine. Therefore, they are

only effective in cells lacking expression of a key urea cycle enzyme, argininosuccinate synthetase 1 (ASS1), which regenerates arginine from citrulline inside the cells [5,6].

Hypoxia in solid tumors is one of the key factor driving malignant progression and therapy resistance. A hypoxic region is formed when a tumor mass outgrows the supplying range of blood vessels. The diffusion barrier causes decreased oxygen levels with increased distance from blood vessels, resulting in continuous or chronic tumor hypoxia. Besides the chronic effect, tumors can also suffer from acute hypoxia caused by collapse of immature vessels or temporary obstructions [7]. In order to survive, tumor cells adapt to the hypoxic environment by regulating expression of stress-response genes [8]. As a result, hypoxic tumors are more resistant to therapies and the surviving cells can act as a foci for tumor relapse, often resulting in poor prognosis [9]. While the role of hypoxia in leading to resistance of tumors to radio- and chemotherapy has been well established [10,11], its effect on arginine depletion strategies has not been investigated.

In this study, we aimed to evaluate ADI-resistance under hypoxic conditions, and also to develop an ADI-delivery system to overcome resistance. Previously, we have shown that intracellular delivery of ADI using a novel cell penetrating peptide (CPP), HBHAc (KKAAPAKKAAAKKAPAKKAAAKK), can restore ADI-treatment sensitivity and enhance therapeutic efficacy in resistant ASS1-expressing cells [12,13]. CPPs are a powerful tool for enabling the intracellular delivery of a wide range of cargo molecules, however their major obstacle in *in vivo* application is their widespread tissue distribution, leading to a low tumor:normal tissue ratio [14]. Therefore, we incorporated our pH-sensitive masking peptide, histidine-glutamic acid (HE) [15–17], into HBHAc-ADI in order to improve its delivery to the tumor cells. Among different tumor targeting mechanisms, pH-sensitive design is ideal for this study since it is well established that tumor hypoxia together with the Warburg effect lead to a mildly acidic tumor microenvironment [18–21]. In order to study the influence of hypoxia on ADI treatment along with pH-sensitive delivery, we designed a mildly acidic hypoxia *in vitro* cell model. The tumor targeted accumulation *in vivo* in a xenograft mouse model of human breast cancer, and pH-sensitive uptake and biological efficacy *in vitro*, of HBHAc-HE-ADI were evaluated.

Materials and Methods

1. Materials

HeLa, MDA-MB-231, and PC3 cells were purchased from ATCC (Manassas, Virginia, USA) and maintained in Roswell Park Memorial Institute (RPMI) 1640 media (HeLa) and Dulbecco's Modified Eagle Medium (DMEM) (MDA-MB-231 and PC3) (Invitrogen, Carlsbad, CA, USA). Restriction enzymes were from New England BioLabs (Ipswich, MA, USA). Sephadex G25 and G50 were from GE healthcare life sciences (Piscataway, NJ, USA). HisPur™ nickel nitriloacetic acid (Ni-NTA) resin was from Thermo Fisher Scientific (Waltham, MA, USA). IRDye® 800CW ("IR800") was from LI-COR Biosciences (Lincoln, NE, USA, USA). Radioactive ^{125}I-Na was from Perkin Elmer (Waltham, MA). Dialysis bags with molecular weight cutoff 12–14 kDa were from Spectrum Laboratories (Rancho Dominguez, CA, USA). Matrigel™ was from BD Biosciences (Bedford, MA, USA). ADI-PEG20 was from Polaris Group (San Diego, CA, USA). pTTQ18-ADI was constructed in

our laboratory as previously described [22] and pUC57 vectors were from Genomics BioSci & Tech (Taipei, Taiwan). Isopropyl β-D-1-thiogalactopyranoside (IPTG) was from Amresco (Solon, OH, USA). Phenylmethylsulfonyl fluoride (PMSF) was from EMD Millipore (Billerica, MA, USA). Fluorescein isothiocyanate (FITC), 3,3′-dihexyloxacarbocyanine iodide (DiOC6), competent *E. coli* BL21-T1^R, protease inhibitor cocktail, Thrombin CleanCleave™ Kit, and other chemicals were from Sigma-Aldrich (St. Louis, MO, USA). Female athymic nude mice (Hsd:Athymic Nude-*Foxn1^{nu}*, 4–6 weeks old) were from Harlan (Livermore, CA, USA).

2. Plasmid construction

The plasmids encoding modified ADI fusion proteins were constructed from pTTQ18-ADI. Each of the peptide sequences, poly-histidine (His_6), His_6-HBHAc and HBHAc-$(HE)_{15}$, were added to the N-terminal of ADI. The His_6 tags and HE repeats which serve as a His-tag [17] were incorporated to enable purification using Ni-NTA agarose chromatography. The His_6 sequences were followed by a thrombin recognition sequence (LVPRGS) to allow for cleavage of the His-tag after production. For HBHAc-$(HE)_{15}$-ADI, a short pentaglycine (G_5) linker was included between HBHAc and $(HE)_{15}$ to obtain flexibility, and the number of HE-repeats (n=15) was selected to obtain an HBHAc-HE sequence with an isoelectric point of 6.8 in order to target the mildly acidic pH region (pH 6.5–7). The DNA sequences of inserts were synthesized and cloned in the pUC57 vector. pTTQ18-ADI and pUC57 encoded inserts were digested with KpnI and SacI, respectively, followed by ligation. The sequences of constructed plasmids were confirmed by colony PCR and sequencing.

3. Protein expression and purification

The correct plasmids were transformed into *E. coli* expression strain BL21. Protein production was induced by adding IPTG. After expression, bacteria were lysed in phosphate buffered saline (PBS) containing 0.1% Triton X-100 and 2 mM PMSF, and following by centrifugation to separate supernatant from inclusion bodies. The undissolved inclusion bodies were washed and dissolved in dissolving buffer (6 M guanidine and 10 mM dithiothreitol in 50 mM Tris buffer). The dissolved protein solution was slowly dropped into 2 L of refolding buffer (1 mM ethylenediaminetetraacetic acid and 0.02% NaN_3 in 10 mM phosphate buffer; for HBHAc-ADI, additional 10 mM arginine was added) with gentle stirring for 48 h at room temperature. After refolding, the aggregates were removed by passing through filter paper followed by concentration using Tangential Flow Filtration (TFF) (Millipore, Billerica, MA, USA). The concentrated fusion proteins were loaded on a Ni-NTA agarose column and then washed with 25 mM imidazole in high salt phosphate buffer (10 mM phosphate and 300 mM NaCl). The fusion proteins were then eluted with high salt phosphate buffer containing 250 mM imidazole. The excess imidazole was removed by dialysis against 10 mM phosphate buffer (pH 7.0). The His-tags were removed by Thrombin CleanCleave™ Kit per the manufacturer's instructions. Briefly, 1 mg of His-tag containing proteins were incubated with 100 μL of thrombin-agarose resin suspension (50% v/v) in 1 mL of cleavage buffer (50 mM Tris-HCl and 10 mM $CaCl_2$, pH 8.0) for 24 h at room temperature. Cleaved fusion proteins were recovered by collecting the supernatant after centrifuging the mixture for 5 min at 500 g. The cleaved His-tags were removed by

dialysis against 10 mM phosphate buffer (pH 7.0). The purity of the fusion proteins was determined by SDS-PAGE followed by Coomassie blue staining.

4. ADI enzyme activity assay

The enzyme activity of ADI fusion proteins was determined by measuring conversion rate of arginine to citrulline using a slightly modified colorimetric citrulline quantification assay [23]. Briefly, 10 μL of ADI or ADI fusion proteins were added into 45 μL of PBS and pre-warmed on a 37 °C dry bath for 5 min. Next, 5 μL of 80 mM arginine was spiked into the protein solution. After incubation at 37 °C for 15 min, the reaction was terminated by the addition of 200 μL color developing reagent (20 mM 2,3-butanedione, 0.5 mM thiosemicarbazide, 2.25 M H_3PO_4, 4.5 M H_2SO_4 and 2 mM $NH_4Fe(SO_4)_2$). Finally, color was developed by heating the mixture in boiling water for 5 min followed by measuring the absorbance at 560 nm. A range of citrulline solutions (6.25 to 400 μM) was used to create a calibration curve, and the amounts of citrulline generated by ADI proteins in 15 min were determined. The enzyme activity per unit is defined as converting 1 μmol arginine to 1 μmol citrulline in 1 min at 37 °C.

5. Labeling of purified proteins

In order to track and quantify protein behavior *in vitro* and *in vivo*, purified protein samples and ADI-PEG20 were labeled with fluorescent dye or radioactive tracer. For *in vitro* cell assays, FITC or ^{125}I was used; for animal imaging study, IR800 was used. The labeling reaction for fluorescent dyes was performed at room temperature for 2 h with a dye/protein molar ratio of 6:1 for FITC and 4:1 for IR800. After the reaction, unlabeled dye was removed using size exclusion chromatography (Sephadex G25) and the labeled fusion proteins were eluted with PBS. For radiolabeling, ^{125}I was conjugated on proteins via the chloramine T method as previously described [24]. The ^{125}I-labeled proteins were purified using size exclusion chromatography (Sephadex G50), the labeled fusion proteins were eluted with PBS, and the radioactivity was determined using a gamma counter (Cora II Auto-Gamma, Packard, Downers Grove, IL, USA).

6. *In vivo* tumor accumulation imaging

All animal studies were performed according to the protocols approved by the University of Southern California Institutional Animal Care and Use Committee. To generate a xenograft model, 7×10^6 MDA-MB-231 cells suspended in 100 μL of Matrigel™ was subcutaneously injected into the right neck region of female athymic nude mice (Hsd:Athymic Nude-*Foxn1*^{nu}, 4–6 weeks old) as previously described [15]. Tumors were allowed to grow to 0.5 to 1 cm^3 in volume before selection for imaging studies. The tumor-bearing mice were separated into two groups (n=3) and injected with IR800-labeled ADI-PEG20 or HBHAc-HE-ADI through tail vein. The *in vivo* tumor accumulation effect was imaged by IVIS SPECTRUM imaging system (PerkinElmer, Waltham, MA, USA) at 0.5, 1, 2, 4 and 6 h post-injection. After the last time point, tumor and organs were collected for *ex vivo* imaging.

7. Hypoxic/normoxic *in vitro* model

An *in vitro* hypoxic cell model was established in order to mimic the mildly acidic environment around hypoxic tumors. MDA-MB-231 or PC3 cells were seeded on 96-well plates with density of 5000 cells/well. After overnight incubation to allow for cell attachment, the culture medium was replaced with modified DMEM containing 50% of the $NaHCO_3$ and L-glutamine concentration (1.85 g/L $NaHCO_3$ and 2 mM L-glutamine) compared to the maintaining medium. The $NaHCO_3$ and L-glutamine concentrations were reduced in order to increase the extracellular acidification rate and buffering capacity, respectively, to mimic the mildly acidic pH microenvironment of tumors [13]. For the hypoxic treatment groups, the cells grown in 96-well plates were transferred to an OxyCycler C42 system (BioSpherix, Redfield, NY, USA) maintained at 0.5% O_2 for MDA-MB-231 or 1% O_2 for PC3 cells, and allowed to balance for 1 day. To avoid fluctuation of oxygen concentration, modified medium was pre-balanced in the respective normoxic or hypoxic incubator overnight before use. The medium pH in both normoxic and hypoxic cultures was measured every 24 h for 72 h.

8. Cellular association and uptake assay

Cell association at different pH was performed in HeLa cells using ^{125}I-labeled fusion proteins. HeLa cells were seeded on 6-well plates at a density of 1×10^6 cells/well one day before assay. Cells were then treated with 5 μg/ml of ^{125}I-labeled fusion proteins prepared in self-made RPMI medium (prepared from RPMI powder, without $NaHCO_3$, with 10 mM Na_2HPO_4 and 10 mM citrate/citric acid) adjusted to pH 6.0, 6.5, 7.0 and 7.5. After 1 h of incubation at 37 °C, cells were washed and detached with trypsin-EDTA. The total cell association, which includes membrane association and internalization, was measured by gamma counter. Cellular uptake of ADI-PEG20 and ADI fusion proteins was also performed on hypoxic/normoxic *in vitro* model.

MDA-MB-231 cells were seeded in 24-well plates at a density of 5×10^4 cells/well and allowed to attach overnight, followed by incubation in either a normoxic or hypoxic incubator for 48 h. FITC labeled proteins (10 μg/mL) were then added to cell monolayers. To avoid influence on pH, sample volume was controlled in less than 1/10 fold of total medium volume. After 1 h of incubation at 37 °C, cells were washed three times with PBS and detached by trypsin-EDTA. Cellular uptake of FITC labeled protein samples was analyzed by flow cytometry (Gallios, Beckman Coulter, Brea, CA, USA)

9. Cytotoxicity assay

The acid phosphatase (ACP) assay, which avoids the effect of mitochondria dysfunction, was used to analyze cytotoxicity. MDA-MB-231 and PC3 cells were seeded on 96-well plates and prepared following the same protocol described in the hypoxic/normoxic *in vitro* model section. After 1 day balance in either normoxic or hypoxic incubator, ADI-PEG20 or ADI fusion proteins were spiked into culture wells at a 10-fold dilution to avoid influence on pH. Cell viability was tested 72 h post-dosing as previously described [25]. Briefly, cells were washed twice with PBS, followed by the addition of 100 μL of 5 mM p-nitrophenol phosphate (p-NPP). The reaction was stopped by the addition of 10 μL of 1N NaOH. Finally, the color change was measured at 410 nm.

10. Mitochondria damage assay

3,3′-Dihexyloxacarbocyanine iodide (DiOC6), a cell-permeant, green-fluorescent lipophilic dye, accumulates in mitochondria due to their large negative membrane potential and is widely used to monitor the mitochondrial membrane potential (MMP) using flow cytometric detection [26–29]. In this study, measurement of MMP was used to detect mitochondria damage. MDA-MB-231 cells were seeded on 24-well plates at a density of 5×10^4 cells/well and treated with 0.3 mU/mL ADI-PEG20 or ADI fusion proteins following the same protocol as the cytotoxicity assay. After 48 h of treatment, cells were harvested and re-suspended in 10 nM of DiOC6. The suspension was incubated at 37 °C for 15 min. Cells were then washed three times with PBS followed by flow cytometry analysis.

11. Statistical Analysis

All values in the manuscript are represented as average value ± standard deviation, and significant differences were evaluated using ANOVA, followed by the Bonferoni modified *t*-test. Differences with a calculated $p < 0.05$ were considered statistically significant, and data were marked with *, ** and *** to indicate $p < 0.05$, $p < 0.01$ and $p < 0.001$, respectively.

Results

1. Hypoxia associated ADI resistance in MDA-MB-231

Human breast cancer MDA-MB-231 cells are ADI sensitive with low ASS1 expression [25]. To evaluate the effect of hypoxia on ADI-sensitivity, cells were treated with 0.0625 to 0.5 mU/mL of ADI-PEG20 under normoxic and hypoxic conditions, and cell viability was measured 72 h after dosing. As shown in Fig. 1A, the half maximal inhibitory concentration (IC_{50}) of ADI-PEG20 increased from 0.25 mU/mL in normoxic condition (21% O_2) to over 0.5 mU/mL in hypoxic condition (0.5% O_2). In addition, it was found that *ASS1* message RNA (mRNA) as well as protein abundance in MDA-MB-231 cells increased following prolonged incubation in hypoxic condition (Fig. 1B).

2. Design and production of ADI fusion proteins

In order to overcome hypoxia-associated ADI resistance, we designed a pH-sensitive HBHAc-HE-ADI fusion protein to achieve targeted intracellular delivery of ADI to the mildly acidic tumor region (Fig. 2A). Unmodified ADI, as well as the HBHAc-ADI fusion protein containing only the CPP sequence without the pH-sensitive masking sequence, served as non-internalizing and non-pH-sensitive controls, respectively (Fig. 2A). After successfully constructing pTTQ18 vectors encoding modified ADI fusion proteins, plasmids were transformed to *E. coli* BL21 strain for protein expression. Corresponding ADI fusion proteins were produced, purified, and analyzed by SDS-PAGE following with Coomassie blue staining. The protein bands showed a gradient position shift from ADI with addition of HBHAc or HBHAc-HE sequences. All three proteins had > 80% purity (Fig. 2B). Among the three proteins, ADI had highest yield of 4 mg, followed by 2.5 mg of HBHAc-HE-ADI and 0.5 mg of HBHAc-ADI, in 500 mL TB culture broth. The enzyme activity of ADI, HBHAc-ADI and HBHAc-HE-ADI was 1.2, 0.6, and 1.2 U/mg, respectively.

3. Cell association at different pH

Next, the pH-sensitive action of HBHAc-HE-ADI was tested on an *in vitro* cell model by adjusting the pH of the cell culture medium to 6.0, 6.5, 7.0 or 7.5 with lactic acid to mimic *in vivo* acidic tumor microenvironment. We used HeLa cells instead of MDA-MB-231 cells for this study due to their higher tolerance to abruptly changing the pH of the extracellular media. As shown in Fig. 2C, the amount of cell-associated ADI was less at all tested pHs, confirming its low binding and internalizing ability [12]. With the assistance of the CPP, HBHAc-ADI showed a higher amount of cell association among all tested pHs. In addition, the association of HBHAc-HE-ADI with cells was pH-dependent. More HBHAc-HE-ADIs were associated with cell at the lower pH than the higher pH. The difference between pH 6.0 and 7.5 was 3.5-fold for HBHAc-HE-ADI and 1.6-fold for HBHAc-ADI, indicating the pH-sensitive action of HBHAc-HE-ADI (Fig. 2C).

4. *In vivo* tumor targeting effect

MDA-MB-231 tumor-bearing nude mice were used to test the *in vivo* pH-sensitive targeting effect of HBHAc-HE-ADI. We first determined if the tumor accumulation of HBHAc-HE-ADI was at least similar to the current clinical ADI formulation, ADI-PEG20. Due to its large molecular size attained by conjugation to approximately ten 20 kDa polyethylene glycol (PEG) chains, ADI-PEG20 accumulated at tumor sites, presumably through the enhanced permeability and retention (EPR) effect [30]. ADI-PEG20 and HBHAc-HE-ADI were labeled with IR800 infrared fluorescent dye before injection into tumor-bearing mice through tail vein. Both HBHAc-HE-ADI and ADI-PEG20 showed a high signal at the tumor region at 30 min post-injection, and the signal intensity was visible for up to 6 h post-injection (Figs. 3A and B). These results indicated that HBHAc-HE-ADI has comparable tumor accumulation effect as ADI-PEG20. However, the *ex vivo* imaging of organs and tumor at 6 h after injection suggested that these two proteins were eliminated through different routes. Apart from the tumor, a high level of ADI-PEG20 was captured in the liver while HBHAc-HE-ADI was detected mainly in the kidneys (Fig. 3C).

5. pH changes and pH-sensitive cellular uptake in normoxic/hypoxic cultured cells

To verify the mildly acidic tumor microenvironment established by hypoxic conditions, the pH of culture media from MDA-MB-231 cells incubated under normoxic (21% O_2) and hypoxic (0.5% O_2) conditions was measured over a period of 72 h incubation. Under hypoxic culture condition, the pH of the medium dropped from 7.6 to 6.7 after 24 h, and continued to decrease to 6.1 after 72 h. The pH of the culture medium under normoxic condition showed a slower decrease, and was maintained at around 7.0 at 48–72 h (Fig. 4A).

After establishing the hypoxic cell culture model to create a mildly acidic environment mimicking *in vivo* tumor conditions, the pH-sensitive cellular uptake of ADI-PEG20 and ADI fusion proteins was determined. FITC-labeled proteins were added to cells 48 h after incubation in normoxic/hypoxic conditions (i.e. the 24 h time point indicated where the medium pH were 7.4 and 6.7, respectively in Fig. 4A). Cellular uptakes of FITC-labeled proteins were measured by flow cytometry after 1 h of incubation. As shown in Fig. 4B, cellular uptakes of ADI-PEG20 and ADI were less in both normoxic and hypoxic conditions. The uptake amount of HBHAc-ADI on the other hand was significantly higher in

both incubation conditions, with only a 1.2-fold difference between normoxic versus hypoxic conditions. In contrast, the uptake of HBHAc-HE-ADI under mildly acidic hypoxic condition was 2.4-fold more than that in the neutral normoxic conditions, indicating the superior pH sensitivity of HBHAc-HE-ADI (Fig. 4B). These results were comparable to those obtained in HeLa cells (Fig. 2C).

6. pH dependent cytotoxicity in normoxic/hypoxic cells

To test the pH dependent cytotoxicity of HBHAc-HE-ADI, MDA-MB-231 cultured in normoxic or hypoxic conditions were treated with 0.0625–0.5 mU/mL of ADI-PEG20, ADI, HBHAc-ADI or HBHAc-HE-ADI. Cell viability was measured at 72 h after dosing. As shown in Fig. 5, both ADI and ADI-PEG20 exhibited similar activity, which was lower in ADI-resistant hypoxic condition (Fig. 5B) compared to normoxic condition (Fig. 5A). With the HBHAc-mediated internalization, HBHAc-ADI showed a dose-dependent, enhanced cytotoxicity under both normoxic and hypoxic conditions (Figs. 5A and B). The cytotoxicity of the pH-sensitive HBHAc-HE-ADI, on the other hand, was comparable to ADI-PEG20 and ADI under normoxic condition (Fig. 5A) where culture medium pH remained neutral (Fig. 4A). However, under the mildly acidic hypoxic condition, the cytotoxicity by HBHAc-HE-ADI increased to the level comparable to that by HBHAc-ADI (Fig. 5B). Similar results were found in PC3, human prostate cancer cells with moderate ASS1 expression [24] at doses ranging from 0.2 to 1 mU/mL (Figs. 6A and B). The mitochondrial damage induced by arginine depletion [25] at 48 h post-dosing was also determined by measuring mitochondrial membrane potential (MMP). Consistent with the cytotoxicity results, HBHAc-HE-ADI caused a higher reduction of MMP under hypoxic condition compared to normoxic condition, where there was no difference from ADI or ADI-PEG20 (Fig. 5C). Together, these results indicated that the mildly acidic pH-dependent delivery of HBHAc-HE-ADI is capable of overcoming ADI-resistance under hypoxic condition. Additionally, the cytotoxicity of ADI or ADI fusion proteins in MCF10A, pseudo-normal immortalized human breast cells, and in peripheral blood mononuclear cells (PBMCs), was minimal **(Supplemental Figs. S1 and S2).**

Discussion

Arginine depletion therapies have become a promising therapeutic approach to treat drug resistant tumors [31]. Multiple types of tumor cells have a defective arginine-to-citrulline pathway due to the suppressed expression of ASS1, thus becoming arginine auxotrophic. As such, depleting extracellular arginine by ADI and its analogs, such as ADI-PEG20, will result in inhibited cell proliferation and eventual cell death [25,32]. However, a major obstacle is that these ADI-sensitive tumor cells could become resistant to arginine deprivation through ASS1 re-expression, thereby converting citrulline to arginine inside cells. The re-expression of ASS1 is regulated by external stimuli in a context-dependent manner. For example, ASS1 expression has been shown to be down-regulated by cisplatin treatment in hepatocarcinoma cell lines [33], while it is up-regulated by arginine deprivation and c-MYC in melanocarcinoma cell lines [34,35]. In this report, we demonstrated that hypoxia, a common feature in solid tumors, is able to induce ASS1 expression in MD-MBA-231 cells, thereby

rendering resistance to arginine deprivation-based therapy in breast cancer cells. Hypoxia-related resistance to ADI was also observed in PC3 prostate cancer cells in this study.

In normal tissues, oxygen levels are generally within a range of 4–7%, but can drop to below 2% in the hypoxic tumor region [36]. In this study, we used a hypoxic incubator with 0.5–1 % of oxygen supply to mimic the tumor hypoxic environment, and evaluated its role in decreasing the effectiveness of ADI. First, we tested the effect of hypoxia on ADI treatment response in the MDA-MB-231 breast cancer cells. We found that hypoxic MDA-MB-231 cells were less sensitive to ADI treatment than their normoxic counterparts (Fig. 1A). This difference in sensitivity in normoxic versus hypoxic conditions was accompanied with an increase in *ASS1* gene expression (Fig. 1B). Although the mechanism underlying hypoxia-induced upregulation of *ASS1* mRNA and ADI resistance in MDA-MB-231 is still unclear, we believe it contributes to the development of resistance to ADI-based therapy. Herein, we aimed at overcoming hypoxia-induced resistance to arginine depletion in general.

The pegylated ADI analog, ADI-PEG20, has been shown to have a good safety profile, and is currently undergoing many Phase I–III clinical trials [31]. However, this drug is not effective in ASS1-expressing cells due to low internalization. Previously, we have shown that a 23-mer CPP, HBHAc, can efficiently deliver ADI into cells to deplete arginine and restore sensitivity of ADI-resistant cells [12]. However, the main concern with CPP-mediated delivery of bioactive cargos *in vivo* is poor biodistribution, leading to a lower accumulation at tumor sites and increased risk of adverse side effects at normal tissues [37]. It is well accepted that both the Warburg effect and the poor vascularization as tumors enlarge will create an acidic tumor microenvironment. Using other CPPs including model amphipathic peptide and oligoarginine, we found that incorporation of an $(HE)_{15}$ co-oligopeptide masking sequence renders a higher binding and uptake of the CPP in cultured cells at the mildly acidic pH 6.5–7 compared to neutral pH 7.4 [15–17](R). We have also shown that the CPP-HE peptides could convey a higher tumor targeting and longer retention *in vivo* using an MDA-MB-231 breast cancer mouse xenograft model [15]. Therefore, we incorporated the HE sequence into HBHAc-ADI to generate a novel pH-activatable HBHAc-HEADI, with improved internalization at the mildly acidic pH (Fig. 2C).

The MDA-MB-231-xenograft tumor bearing mice have previously been shown to be suitable for testing pH-sensitive targeting effect [15]. The tumor targeting mechanism of HBHAc-HE-ADI depends on pH-sensitive unmasking of the HE sequence, while the current product, ADI-PEG20, is presumably based on the EPR effect as it has been reported that particles ranging from 10 to 100 nm in size or with a molecular weight lager than 60 kDa tend to accumulate inside tumors through the immature, leaky blood vessels [38]. In ADI-PEG20, there are at least 10 PEGs (20 kDa each) attached, which brings the size up to around 250 kDa [39]. The *in vivo* imaging showed that our HBHAc-HE-ADI exhibited a comparable tumor accumulation as ADI-PEG20 (Fig. 3). However, these two proteins utilized different elimination routes. HBHAc-HEADI was mainly distributed to kidney due to the smaller size of 54 kDa, which is slightly lower than renal filtration cutoff size of 60 kDa [35]. Pegylation is a well-established method to enlarge molecular size to avoid renal filtration. Previous reports have shown that renal accumulation is sharply decreased with the modification of PEG size larger than 5 kDa [21]. Therefore, ADI-PEG20 exhibits a relatively low signal in the kidney,

but was instead eliminated mainly via the liver (Fig. 3C). This result was not surprising since the enlarged size of ADI-PEG20 is expected to cause greater uptake by the reticuloendothelial system (RES) in liver, which is responsible for macromolecule clearance [40].

In order to adapt to the hypoxic environment, tumor cells further exacerbate their Warburg metabolic phenotype by accelerating glucose uptake and glycolysis rates, which leads to increased lactic acid production and results in acidification of the extracellular environment [21]. We observed a much faster acidification of the culture medium when MDA-MB-231 cells were cultured in a hypoxic environment than when maintained in a normoxic incubator. In order to study the *in vitro* pH-dependency of HBHAc-HE-ADI in MDA-MB-231 cells, a hypoxic exposure was utilized to generate a condition resembling the acidic tumor microenvironment. Consistent with the results in HeLa cells (Fig. 2C) and our previous studies [12], ADI-PEG20 and ADI showed low cell internalization, while HBHAc-ADI showed high internalization, in both normoxic and hypoxic culture conditions. HBHAc-HE-ADI showed a pH-dependent cell internalization, with low uptake in normoxic cells (neutral pH) and high uptake in hypoxic cells (mildly acidic) (Fig. 4B). In summary, HBHAc-HE-ADI reproducibly exhibited pH-dependency in both HeLa and MDA-MB-231 cells compared to HBHAc-ADI (Figs. 2C and 4B).

Next, the ADI-induced cytotoxicity was tested in our normoxic/hypoxic MDA-MB-231 and PC3 cell models (Figs. 5 and 6). Due to their inability to deplete intracellular arginine, ADI and ADI-PEG20 had lower cytotoxic effect in hypoxic cells, in which the *ASS1* expression was induced. In contrast, the efficacy of HBHAc-ADI, with its ability of extra- and intracellular arginine depletion as well as its high internalization at both mildly acidic (hypoxic) and neutral (normoxic) pH, was not affected by O_2 tension. The pH-sensitive delivery of HBHAc-HE-ADI (Figs. 2C and 4B), on the other hand, provided hypoxia-associated, pH-dependent cytotoxicity in both cell viability and mitochondria integrity assays (Figs. 5 and 6). Therefore, compared to the lack of selectivity HBHAc-ADI at different pH, HBHAc-HE-ADI shows pH-sensitive activity only in the mildly acidic pH seen in tumor microenvironments, and was inactive at neutral pH conditions at the surface of normal tissues. Thus, this pH-selective activity further minimizes the potential for undesired toxic side effects. Further, the pH-dependent targeting can also potentially improve the biodistribution of the protein drug by enhancing its delivery and/or retention at the tumor site. Interestingly, although the cellular uptake of HBHAc-ADI in normoxic and hypoxic MDA-MB-231 cells was much higher than HBHAc-HE-ADI (Fig. 4B), it did not lead to a significant enhancement in its cytotoxicity (Fig. 5). It is possible that only a small portion of ADI from the fusion protein could escape from endosomes, resulting in a comparable cytotoxicity of HBHAc-ADI and HBHAc-HE-ADI under hypoxia. Further, histidine residues in HE oligopeptide may facilitate the endosomal escape of HBHAc-HE-ADI [41,42], resulting in a larger proportion localized in the cytosol when compared to HBHAc-ADI.

Conclusion

In this report, we showed that hypoxic conditions can induce ADI-resistance through increased expression of ASS1. The intracellular delivery of ADI via HBHAc could be a

useful strategy to overcome the hypoxia-induced resistance in breast and prostate cancer cells. Our pH-sensitive HBHAc-HE-ADI showed a favorable accumulation in xenografted tumors *in vivo* and increased *in vitro* tumor cellular uptake in the mildly acidic pH 6.5 compared to neutral pH 7.4. The pH-dependent internalization led to increased cytotoxicity only in hypoxic cells with a mildly acidic extracellular pH, while the activity was lower and comparable to the non-internalizing ADI and ADI-PEG20 in normoxic cells with a neutral extracellular pH. The pH-sensitive internalization and activity of HBHAC-HE-ADI provides the ability to target this biomolecule specifically to the mildly acidic pH tumor microenvironment *in vivo*. Therefore, HBHAc-HE-ADI fusion protein with pH-sensitive tumor targeted internalization offers a novel treatment strategy to overcome ADI-resistance induced by hypoxia, which is frequently encountered in many solid tumors, and is expected to improve treatment efficacy.

Acknowledgments

Funding Sources

This work was supported in part by grants to LJS, JLZ and DKA from the National Science Council of Taiwan (NSC 100-2320-B-002-007-MY3), the NIH National Cancer Institute (R21CA169841 and P30CA33572), and the Mary Kay Foundation (005-13). THY was a visiting graduate student at the University of Southern California (USC) from National Taiwan University. She was supported by *Graduate Student Study Abroad* Program (102-2917-I-002-007) from the National Science Council, Taiwan.

We would like to thank Dr. Likun Fei from the USC School of Pharmacy and Dr. Li-Peng Yap at the USC Molecular Imaging Center for assistance with establishing the mouse xenograft models and the animal imaging studies.

ABBREVIATIONS

ADI	arginine deiminase
ADI-PEG20	pegylated recombinant arginine deiminase
ASS1	argininosuccinate synthetase 1
CPP	cell penetrating peptide
HE	histidine-glutamine
HIF-1	hypoxia-inducible factor-1

References

1. Shen LJ, Shen WC. Drug evaluation: ADI-PEG-20--a PEGylated arginine deiminase for arginine-auxotrophic cancers. Curr Opin Mol Ther. 2006; 8:240–248. [PubMed: 16774044]
2. Ott PA, Carvajal RD, Pandit-Taskar N, Jungbluth AA, Hoffman EW, Wu BW, Bomalaski JS, Venhaus R, Pan L, Old LJ, Pavlick AC, Wolchok JD. Phase I/II study of pegylated arginine deiminase (ADI-PEG 20) in patients with advanced melanoma. Invest New Drugs. 2013; 31:425–434. [PubMed: 22864522]
3. Yang TS, Lu SN, Chao Y, Sheen IS, Lin CC, Wang TE, Chen SC, Wang JH, Liao LY, Thomson JA, Wang-Peng J, Chen PJ, Chen LT. A randomised phase II study of pegylated arginine deiminase (ADI-PEG 20) in Asian advanced hepatocellular carcinoma patients. Br J Cancer. 2010; 103:954–960. [PubMed: 20808309]

4. Glazer ES, Piccirillo M, Albino V, Di Giacomo R, Palaia R, Mastro AA, Beneduce G, Castello G, De Rosa V, Petrillo A, Ascierto PA, Curley SA, Izzo F. Phase II study of pegylated arginine deiminase for nonresectable and metastatic hepatocellular carcinoma. J Clin Oncol. 2010; 28:2220–2226. [PubMed: 20351325]
5. Shen LJ, Lin WC, Beloussow K, Shen WC. Resistance to the anti-proliferative activity of recombinant arginine deiminase in cell culture correlates with the endogenous enzyme, argininosuccinate synthetase. Cancer Lett. 2003; 191:165–170. [PubMed: 12618329]
6. Shen LJ, Beloussow K, Shen WC. Modulation of arginine metabolic pathways as the potential anti-tumor mechanism of recombinant arginine deiminase. Cancer Lett. 2006; 231:30–35. [PubMed: 16356828]
7. Kizaka-Kondoh S, Inoue M, Harada H, Hiraoka M. Tumor hypoxia: a target for selective cancer therapy. Cancer Sci. 2003; 94:1021–1028. [PubMed: 14662015]
8. Semenza GL. Hypoxia-inducible factors: mediators of cancer progression and targets for cancer therapy. Trends Pharmacol Sci. 2012; 33:207–214. [PubMed: 22398146]
9. Mayer A, Vaupel P. Hypoxia, lactate accumulation, and acidosis: siblings or accomplices driving tumor progression and resistance to therapy? Adv Exp Med Biol. 2013; 789:203–209. [PubMed: 23852496]
10. Willers H, Azzoli CG, Santivasi WL, Xia F. Basic mechanisms of therapeutic resistance to radiation and chemotherapy in lung cancer. Cancer J. 2013; 19:200–207. [PubMed: 23708066]
11. Rohwer N, Cramer T. Hypoxia-mediated drug resistance: novel insights on the functional interaction of HIFs and cell death pathways. Drug Resist Updat. 2011; 14:191–201. [PubMed: 21466972]
12. Wu FL, Yeh TH, Chen YL, Chiu YC, Cheng JC, Wei MF, Shen LJ. Intracellular delivery of recombinant arginine deiminase (rADI) by heparin-binding hemagglutinin adhesion peptide restores sensitivity in rADI-resistant cancer cells. Mol Pharm. 2014; 11:2777–2786. [PubMed: 24950134]
13. Lin TC, Chen YR, Kensicki E, Li AY, Kong M, Li Y, Mohney RP, Shen HM, Stiles B, Mizushima N, Lin LI, Ann DK. Autophagy: resetting glutamine-dependent metabolism and oxygen consumption. Autophagy. 2012; 8:1477–1493. [PubMed: 22906967]
14. Sarko D, Beijer B, Garcia Boy R, Nothelfer EM, Leotta K, Eisenhut M, Altmann A, Haberkorn U, Mier W. The pharmacokinetics of cell-penetrating peptides. Mol Pharm. 2010; 7:2224–2231. [PubMed: 20845937]
15. Fei L, Yap LP, Conti PS, Shen WC, Zaro JL. Tumor targeting of a cell penetrating peptide by fusing with a pH-sensitive histidine-glutamate co-oligopeptide. Biomaterials. 2014; 35:4082–4087. [PubMed: 24508076]
16. Sun C, Shen WC, Tu J, Zaro JL. Interaction between cell-penetrating peptides and acid-sensitive anionic oligopeptides as a model for the design of targeted drug carriers. Mol Pharm. 2014; 11:1583–1590. [PubMed: 24697211]
17. Zaro JL, Fei L, Shen WC. Recombinant peptide constructs for targeted cell penetrating peptide-mediated delivery. J Control Release. 2012; 158:357–361. [PubMed: 22326404]
18. Warburg O. On the origin of cancer cells. Science. 1956; 123:309–314. [PubMed: 13298683]
19. Stubbs M, Bashford CL, Griffiths JR. Understanding the tumor metabolic phenotype in the genomic era. Curr Mol Med. 2003; 3:49–59. [PubMed: 12558074]
20. Semenza GL. Targeting HIF-1 for cancer therapy. Nat Rev Cancer. 2003; 3:721–732. [PubMed: 13130303]
21. Brahimi-Horn MC, Pouyssegur J. Hypoxia in cancer cell metabolism and pH regulation. Essays Biochem. 2007; 43:165–178. [PubMed: 17705800]
22. Beloussow K, Wang L, Wu J, Ann D, Shen WC. Recombinant arginine deiminase as a potential anti-angiogenic agent. Cancer Lett. 2002; 183:155–162. [PubMed: 12065090]
23. Nicklin SA, Dishart KL, Buening H, Reynolds PN, Hallek M, Nemerow GR, Von Seggern DJ, Baker AH. Transductional and transcriptional targeting of cancer cells using genetically engineered viral vectors. Cancer Lett. 2003; 201:165–173. [PubMed: 14607330]
24. Kim RH, Coates JM, Bowles TL, McNerney GP, Sutcliffe J, Jung JU, Gandour-Edwards R, Chuang FY, Bold RJ, Kung HJ. Arginine deiminase as a novel therapy for prostate cancer induces

autophagy and caspase-independent apoptosis. Cancer research. 2009; 69:700–708. [PubMed: 19147587]

25. Qiu F, Chen YR, Liu X, Chu CY, Shen LJ, Xu J, Gaur S, Forman HJ, Zhang H, Zheng S, Yen Y, Huang J, Kung HJ, Ann DK. Arginine starvation impairs mitochondrial respiratory function in ASS1-deficient breast cancer cells. Sci Signal. 2014; 7:ra31. [PubMed: 24692592]
26. Korchak HM, Rich AM, Wilkenfeld C, Rutherford LE, Weissmann G. A carbocyanine dye, DiOC6(3), acts as a mitochondrial probe in human neutrophils. Biochem Biophys Res Commun. 1982; 108:1495–1501. [PubMed: 7181903]
27. Tedeschi H. Mitochondrial membrane potential: evidence from studies with a fluorescent probe. Proc Natl Acad Sci U S A. 1974; 71:583–585. [PubMed: 4521825]
28. Rottenberg H, Wu S. Quantitative assay by flow cytometry of the mitochondrial membrane potential in intact cells. Biochim Biophys Acta. 1998; 1404:393–404. [PubMed: 9739168]
29. Marchetti P, Castedo M, Susin SA, Zamzami N, Hirsch T, Macho A, Haeffner A, Hirsch F, Geuskens M, Kroemer G. Mitochondrial permeability transition is a central coordinating event of apoptosis. J Exp Med. 1996; 184:1155–1160. [PubMed: 9064332]
30. Bailon P, Won CY. PEG-modified biopharmaceuticals. Expert Opin Drug Deliv. 2009; 6:1–16. [PubMed: 19236204]
31. Phillips MM, Sheaff MT, Szlosarek PW. Targeting arginine-dependent cancers with arginine-degrading enzymes: opportunities and challenges. Cancer Res Treat. 2013; 45:251–262. [PubMed: 24453997]
32. Changou CA, Chen YR, Xing L, Yen Y, Chuang FY, Cheng RH, Bold RJ, Ann DK, Kung HJ. Arginine starvation-associated atypical cellular death involves mitochondrial dysfunction, nuclear DNA leakage, and chromatin autophagy. Proc Natl Acad Sci U S A. 2014; 111:14147–14152. [PubMed: 25122679]
33. McAlpine JA, Lu HT, Wu KC, Knowles SK, Thomson JA. Down-regulation of argininosuccinate synthetase is associated with cisplatin resistance in hepatocellular carcinoma cell lines: implications for PEGylated arginine deiminase combination therapy. BMC Cancer. 2014; 14:621. [PubMed: 25164070]
34. Long Y, Tsai WB, Wangpaichitr M, Tsukamoto T, Savaraj N, Feun LG, Kuo MT. Arginine deiminase resistance in melanoma cells is associated with metabolic reprogramming, glucose dependence, and glutamine addiction. Mol Cancer Ther. 2013; 12:2581–2590. [PubMed: 23979920]
35. Tsai WB, Aiba I, Lee SY, Feun L, Savaraj N, Kuo MT. Resistance to arginine deiminase treatment in melanoma cells is associated with induced argininosuccinate synthetase expression involving c-Myc/HIF-1alpha/Sp4. Mol Cancer Ther. 2009; 8:3223–3233. [PubMed: 19934275]
36. Brown JM, Wilson WR. Exploiting tumour hypoxia in cancer treatment. Nat Rev Cancer. 2004; 4:437–447. [PubMed: 15170446]
37. Koren E, Torchilin VP. Cell-penetrating peptides: breaking through to the other side. Trends Mol Med. 2012; 18:385–393. [PubMed: 22682515]
38. Fang J, Sawa T, Maeda H. Factors and mechanism of “EPR” effect and the enhanced antitumor effects of macromolecular drugs including SMANCS. Adv Exp Med Biol. 2003; 519:29–49. [PubMed: 12675206]
39. Belani CP, Yamamoto N, Bondarenko IM, Poltoratskiy A, Novello S, Tang J, Bycott P, Niethammer AG, Ingrosso A, Kim S, Scagliotti GV. Randomized phase II study of pemetrexed/cisplatin with or without axitinib for non-squamous non-small-cell lung cancer. BMC Cancer. 2014; 14:290. [PubMed: 24766732]
40. Sadauskas E, Wallin H, Stoltenberg M, Vogel U, Doering P, Larsen A, Danscher G. Kupffer cells are central in the removal of nanoparticles from the organism. Part Fibre Toxicol. 2007; 4:10. [PubMed: 17949501]
41. Erazo-Oliveras A, Muthukrishnan N, Baker R, Wang TY, Pellois JP. Improving the endosomal escape of cell-penetrating peptides and their cargos: strategies and challenges. Pharmaceuticals (Basel). 2012; 5:1177–1209. [PubMed: 24223492]

42. Lo SL, Wang S. An endosomolytic Tat peptide produced by incorporation of histidine and cysteine residues as a nonviral vector for DNA transfection. Biomaterials. 2008; 29:2408–2414. [PubMed: 18295328]

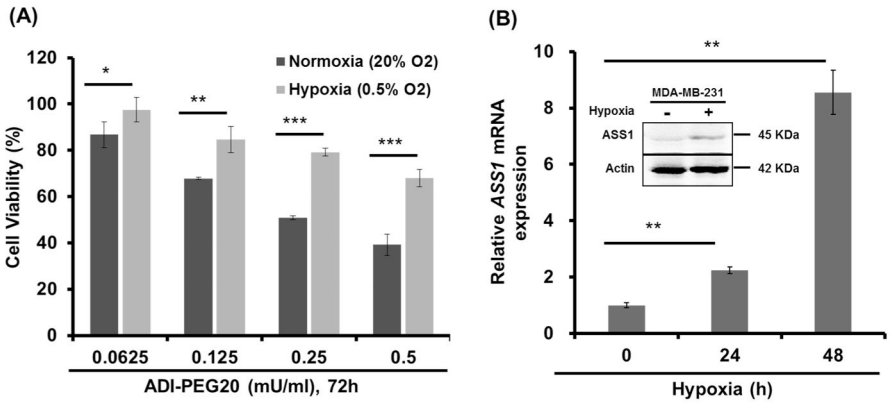

Fig. 1. Hypoxia-associated ADI resistance in MDA-MB-231 cells

(A) MDA-MB-231 cells cultured in hypoxic 0.5% O_2 showed resistance to ADI treatment compared to normoxic 21% O_2. Cells were treated with ADI-PEG20 for 72 h. (B) Hypoxia induces *ASS1* mRNA and protein expression. MDA-MB-231 cells were cultured under hypoxic conditions (0.5% O_2) for the indicated time periods. *Inset:* MDA-MB-231 cell lysates were analyzed by SDS-PAGE followed by anti-ASS1 and anti-Actin Western blot. (A–B) Bars represent average values with error bars indicating standard deviation (n = 3). Bars marked with *, ** and *** indicate $p < 0.05$, $p < 0.01$ and $p < 0.001$, respectively, as determined using the Bonferoni modified *t*-test.

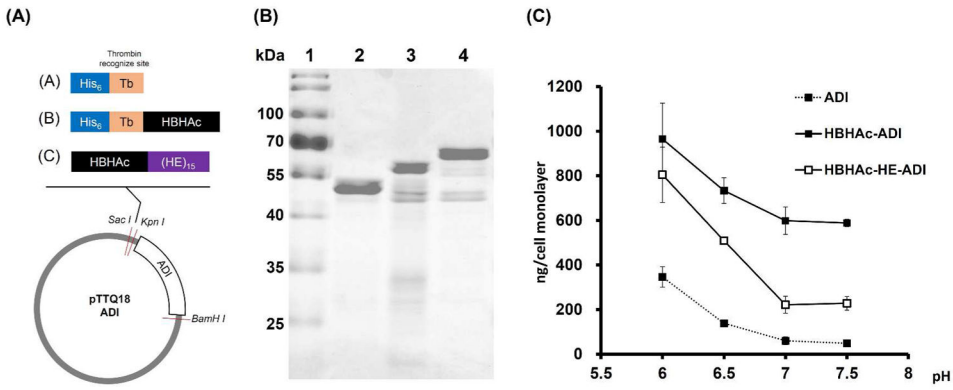

Fig. 2. Design, production and characterization of ADI fusion proteins

(A) Construct design of ADI fusion proteins. Modified sequences were inserted into pTTQ18-ADI vector. (B) Production of ADI fusion proteins. The purified proteins were analyzed by Coomassie blue staining. Lane 1: Protein ladder; Lane 2: ADI; Lane 3: HBHAc-ADI; Lane 4: HBHAc-HE-ADI. (C) pH-dependent cell association of ADI fusion proteins. ^{125}I-labeled ADI (closed squares, dashed line), HBHAc-ADI (closed squares, solid line) or HBHAc-HE-ADI (open squares, solid line) (5 μg/ml) were added to HeLa cells incubated at the indicated extracellular pH and the cell association was measured after 1 h of incubation. Data points represent average values with error bars indicating standard deviation (n = 3).

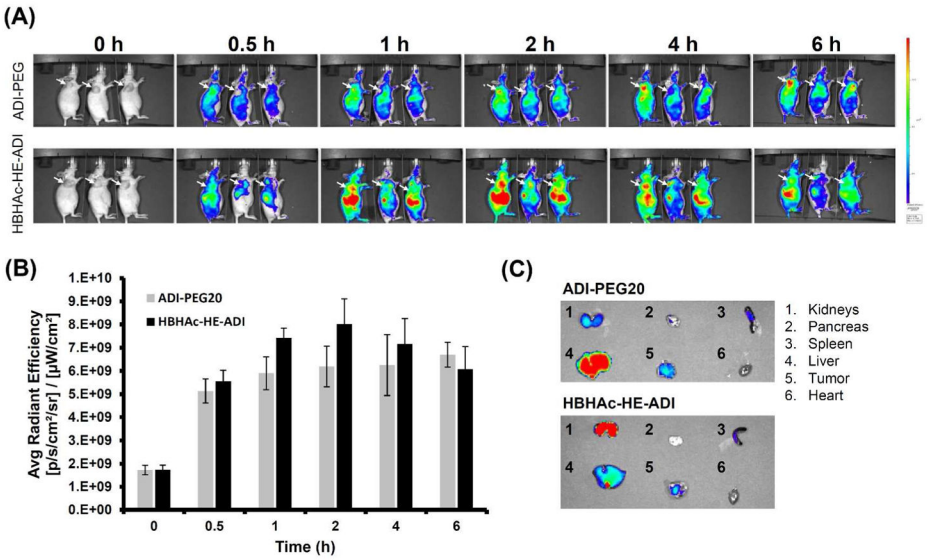

Fig. 3. ***In vivo*** **tumor targeting effect**

IR800 labeled ADI-PEG20 and HBHAc-HE-ADI were injected to MDA-MB-231 tumor-bearing nude mice through tail vein. (A) Biodistribution imaging was captured post-injection at indicated time points. White arrows indicate tumor region. (B) Signal intensity at tumor region was quantified. Bars represent average values with error bars indicating standard deviation (n = 3). (C) *Ex vivo* imaging of organs and tumor was performed 6 h post-injection.

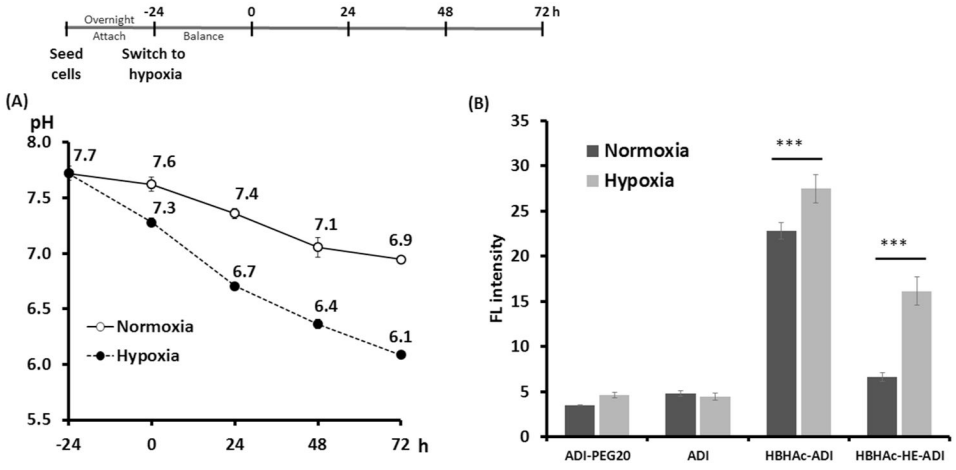

Fig. 4. Effect of normoxic and hypoxic incubation conditions on pH of extracellular medium and on cellular uptake of FITC labeled protein

(A) MDA-MB-231 cells were cultured in a normoxic (21% O_2) or a hypoxic incubator (0.5% O_2), and the pH of the culture medium was measured at the indicated time points. Data points represent average with error bars indicating standard deviation (n = 3). (B) FITC labeled ADI-PEG20 and ADI fusion proteins were added to the cells 48 h after incubation in normoxic/hypoxic conditions. After 1 h of incubation, cellular uptake was measured by flow cytometry and quantified by FL intensity. Bars represent average values with error bars indicating standard deviation (n = 3). Bars marked as *** indicate $p < 0.001$ as determined using the Bonferoni modified t-test.

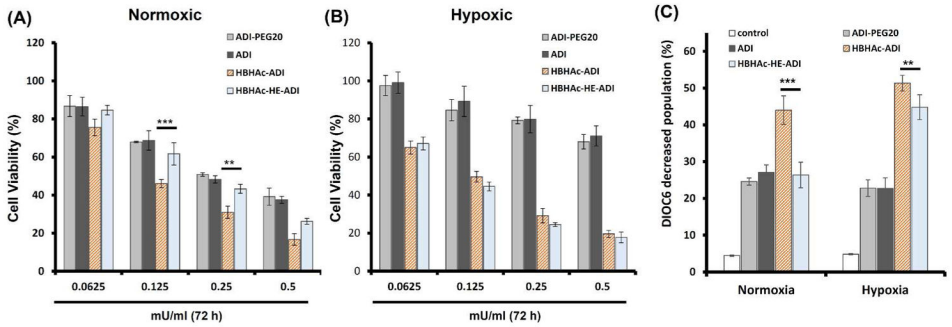

Fig. 5. Bioactivity of ADI-fusion proteins in MDA-MB-231 cells under normoxic and hypoxic conditions

MDA-MB-231 cells cultured under hypoxic or normoxic conditions were treated with ADI-PEG20 or ADI fusion proteins. (A) Normoxic cell viability and (B) hypoxic cell viability were measured at 72 h post-dosing. (C) Mitochondria function was determined at 48 h post-dosing. Cells treated with PBS were used as a control. Bars represent average values with error bars indicating standard deviation (n = 3). (A–C) Bars marked as ** and *** indicate $p < 0.01$ and $p < 0.001$, respectively, as determined using the Bonferoni modified t-test.

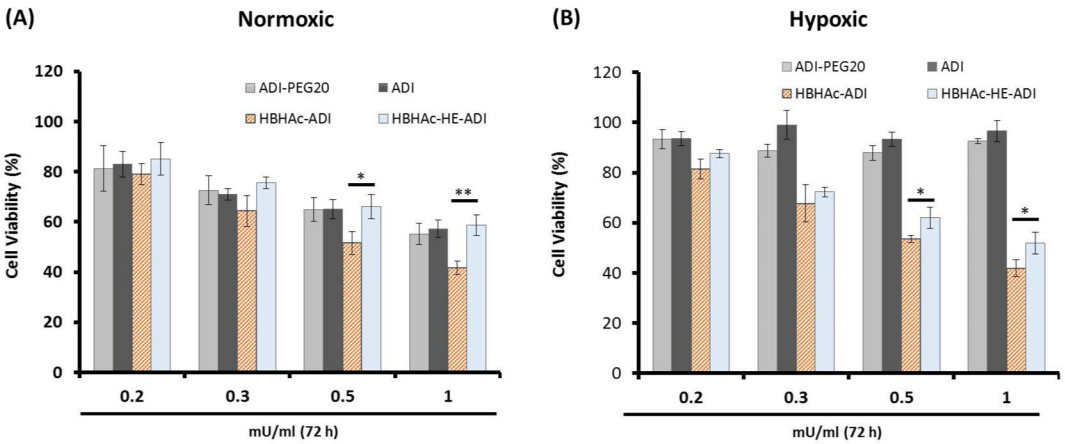

Fig. 6. Bioactivity of ADI-fusion proteins in PC3 cells under normoxic and hypoxic conditions

PC3 cells cultured under hypoxic or normoxic conditions were treated with ADI-PEG20 or ADI fusion proteins. (A) Normoxic cell viability and (B) hypoxic cell viability were measured at 72 h post-dosing. Bars represent average values with error bars indicating standard deviation (n = 3). Bars marked as * and ** indicate $p < 0.05$ and $p < 0.01$, respectively, as determined using the Bonferoni modified t-test.